Geometric properties of anthropogenic flood control berms on southern California beaches

T.W. Gallien [a, *], W.C. O'Reilly [a], R.E. Flick [b], R.T. Guza [a]

[a] Scripps Institution of Oceanography, University of California, San Diego, United States
[b] California Department of Parks and Recreation, Division of Boating and Waterways, United States

ABSTRACT

Coastal flood risk from coincident high tides and energetic waves is concentrated around low-lying urban areas. Municipalities construct temporary sand berms (also known as sacrificial dunes) to manage potential flooding, however the relationships between berm geometry (e.g., height, width and length) and performance are not understood. Concomitant pressures of sea level rise and urbanization will increase active beach berming. Effective future coastal flood risk management will depend upon optimizing berm efficacy relative to geometry, placement, and water levels. Here, 34 individual berms at seven southern California locations are characterized using 18 LiDAR datasets spanning nearly a decade. Three berm classifications emerged based on deployment duration: event, seasonal and persistent. Event berms, deployed to manage specific storms or high water events, are triangular in cross-section, relatively low volume (~4 m^3/m) and low crest elevation (~5 m NAVD88). Seasonal berms are larger, volumes vary from 6 to 28 m^3/m, and average crest elevations are between 5.3 and 6.4 m. A persistent berm, captured in all LiDAR data for that area, is the largest (48 m^3/m), longest (1.2 km), and highest mean crest elevation (7 m NAVD88) of all study berms. Total water levels, estimated using observed tides and a regional wave model coupled with an empirical runup formula, suggest that overtopping is rare. Currently, event berms are vulnerable to wave attack only a few hours per year. However, even with modest sea level rise (~25 cm) or El Niño conditions, exposure increases significantly, and substantial nourishments may be required to maintain current flood protection levels.

© 2014 Elsevier Ltd. All rights reserved.

1. Introduction

Urban coastal flooding is a global humanitarian and socioeconomic hazard. Over 20 million people reside below present day high tide levels, and 200 million are vulnerable to storm flooding (Nicholls, 2011). Sea level rise will substantially increase risks to human life and infrastructure (e.g., Hanson et al., 2011). In the context of coastal risk management, three prevailing options for addressing present and future flooding are to protect, accommodate or retreat (Linham and Nicholls, 2012). Although new development may be built to accommodate high water conditions, economically valuable legacy structures require protection. Hard armoring can increase passive erosion, damage ecosystems and limit recreation (e.g., Airoldi et al., 2005; Martin et al., 2005;

Pendleton et al., 2012). Soft protection such as beach nourishment or artificial dune construction (e.g. Flick, 1993; Rogers et al., 2010; Cooke et al., 2012; Cooper and Lemckert, 2012; Pendleton et al., 2012) may be preferred in locations where beaches are central to culture and economy.

Extensive research efforts have considered the protective effects of beach nourishments (e.g., National Research Council, 1995; Dean, 2001; Hanson et al., 2002) and coastal dunes (e.g., van Rijn, 2009; Bochev et al., 2011; El Mrini et al., 2012; Hanley et al., 2014). van Rijn (2011) assessed the effectiveness of hard and soft erosion management practices on sandy beaches using a mix of numerical modeling, laboratory and field data. Matias et al. (2005) studied dune nourishment along an eroded barrier island and concluded that augmented natural dunes successfully mitigated overwash events. Sallenger (2000) developed a storm impact scale to assess dune vulnerability and Judge et al. (2003) proposed survival and failure indication parameters. Dune erosion modeling has received significant and sustained attention (e.g., Edelman, 1968, 1972; van de Graff, 1977; Vellinga, 1982; Fisher and Overton, 1985; Kriebel

and Dean, 1985; Kobayashi, 1987; Kriebel, 1991; Overton et al., 1994; Sallenger, 2000; Erikson et al., 2007; Roelvink et al., 2009). Edelman (1968, 1972), Kobayashi (1987); Kriebel (1991) and Larson et al. (2004) developed simple analytical dune erosion models. Larson and Kraus (1989) presented SBEACH, an empirically based numerical model and Roelvink et al. (2009) developed a two dimensional flow and sediment transport model, XBeach, for predicting cross-shore beach evolution. Collectively, this work shows the beach-dune system's coastal protection utility. However, these studies do not examine artificial dunes constructed specifically to mitigate imminent coastal flooding hazards.

Beach berming, also known as beach scraping, bumping, re-profiling, and nature assisted beach enhancement (NABE), is the mechanical transfer of a thin layer of sand from the lower beach foreshore to the beach crest (Bruun, 1983) that originated primarily as an erosion control method (e.g., Bruun, 1983; Tye, 1983; Wells and McNinch, 1991; McNinch and Wells, 1992). In contrast to permanent dike structures found in continuously vulnerable regions such as the Netherlands, these berms are often sacrificial, intended only to deflect specific high water or energetic wave events. Temporary berming is a widely used coastal management strategy along the US coasts (e.g., Wells and McNinch, 1991; Clark, 2005; Kratzmann and Hapke, 2012), Australia (Carley et al., 2010) and Europe (e.g., Rogers et al., 2010; Harley and Ciavola, 2013). Kana and Svetlichny (1982) monitored a 14 km berming project along the US East Coast and found that beach berming provided relatively limited erosion protection. Froede (2010) concluded that although berms constructed on a barrier-spit island eroded in 15–27 months, they are integral to residential development protection. Recently beach berming has been used to mitigate flood risk (e.g., Harley and Ciavola, 2013). In California, Edge et al. (2003) recognized the importance of beach berms for seasonal coastal protection and Schubert et al. (in press) studied prototype flood control

berm failures. Extensive studies of artificial dunes in Fire Island, New York (Kratzmann and Hapke, 2012) and Florida (Magliocca et al., 2011) focused on the morphodynamic consequences on adjacent beaches rather than on the berms themselves. Hanley et al. (2014) considered the effects of winter dune construction on macro-invertebrate population at heavily managed beaches along the Adriatic Coast, but did not geometrically characterize the temporary dunes. Finally, Harley and Ciavola (2013) recognized the importance of artificial dunes protecting flood prone stretches of the Emilia-Romanga coast in Northern Italy and proposed a design tool, DuneMaker, to integrate berm geometries into a hydro-morphological model. Clearly, beach berms play an important role in proactive coastal flood management. Near term sea level rise mitigation and adaptation strategies will increase berming activities, however fundamental berm design and performance data is absent in the literature. Understanding berm efficacy is crucial to optimal future beach management.

Laser scanning, also known as LiDAR has been widely used to characterize both urban infrastructure and beach sand levels (e.g., Brock et al., 2002; Sallenger et al., 2003; Sanders, 2007; Fewtrell et al., 2011; Gallien et al., 2011). Pietro et al. (2008) and Gares et al. (2006) monitored beach nourishment using LiDAR whereas Feagin et al. (2014) monitored dune volume change. Stockdon et al. (2002) used LiDAR to estimate shoreline change and extract dune crest elevations while Kratzmann and Hapke (2012) studied morphological consequences from berm building. In California, LiDAR has been used to estimate levee stability (Casas et al., 2012), cliff erosion (e.g., Young and Ashford, 2006; Young et al., 2011) and seasonal sand level changes (Yates et al., 2009). Here, a decade of southern California coastal LiDAR is used to locate and quantitatively characterize anthropogenic flood control berms ranging from small ad-hoc event specific berms (Fig. 1a,b,d) built in hours or days before a storm event, annual seasonal berms (Fig. 1c) to large sand
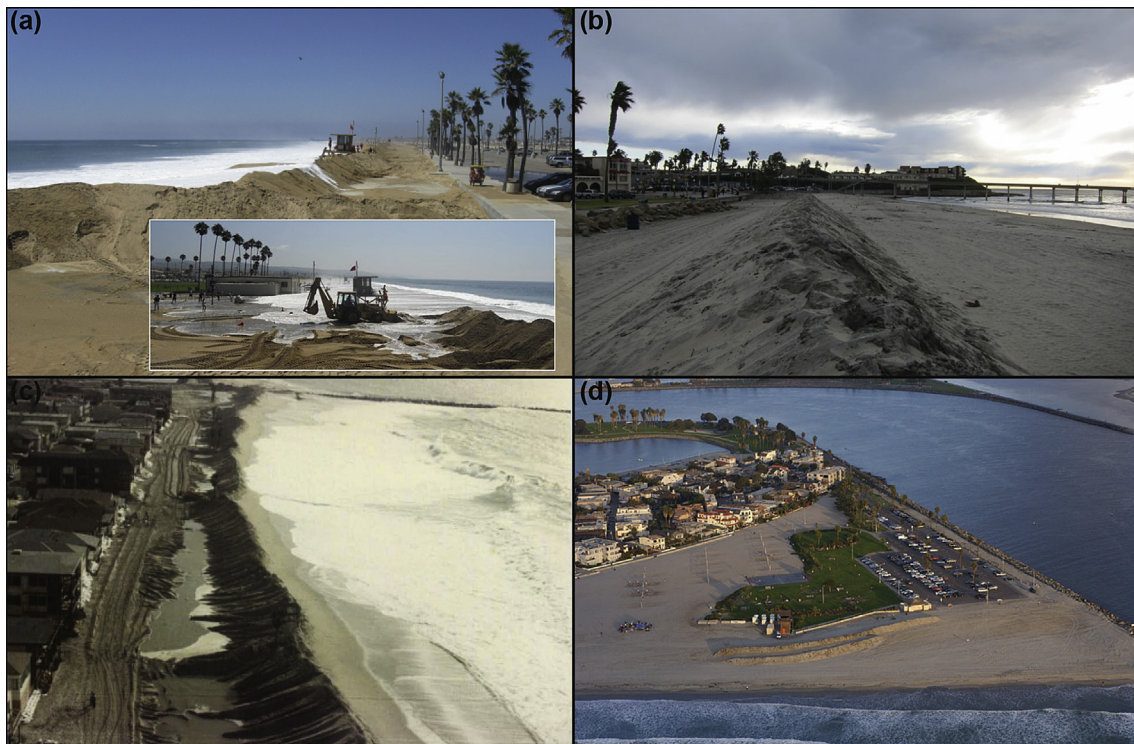

Fig. 1. Examples of anthropogenic beach berms at (a) Balboa Beach August, 2011, inset photo shows end flow around the berm edge (b) Ocean Beach December, 2011 (photo used with permission, George Fatell) (c) Seal Beach, 1983 (McMahon, 2009) and (d) Mission Beach, October 2006, photo used with permission, ©2002–2013 Kenneth and Gabrielle Adelman, California Coastal Records Project www.Californiacoastline.org.
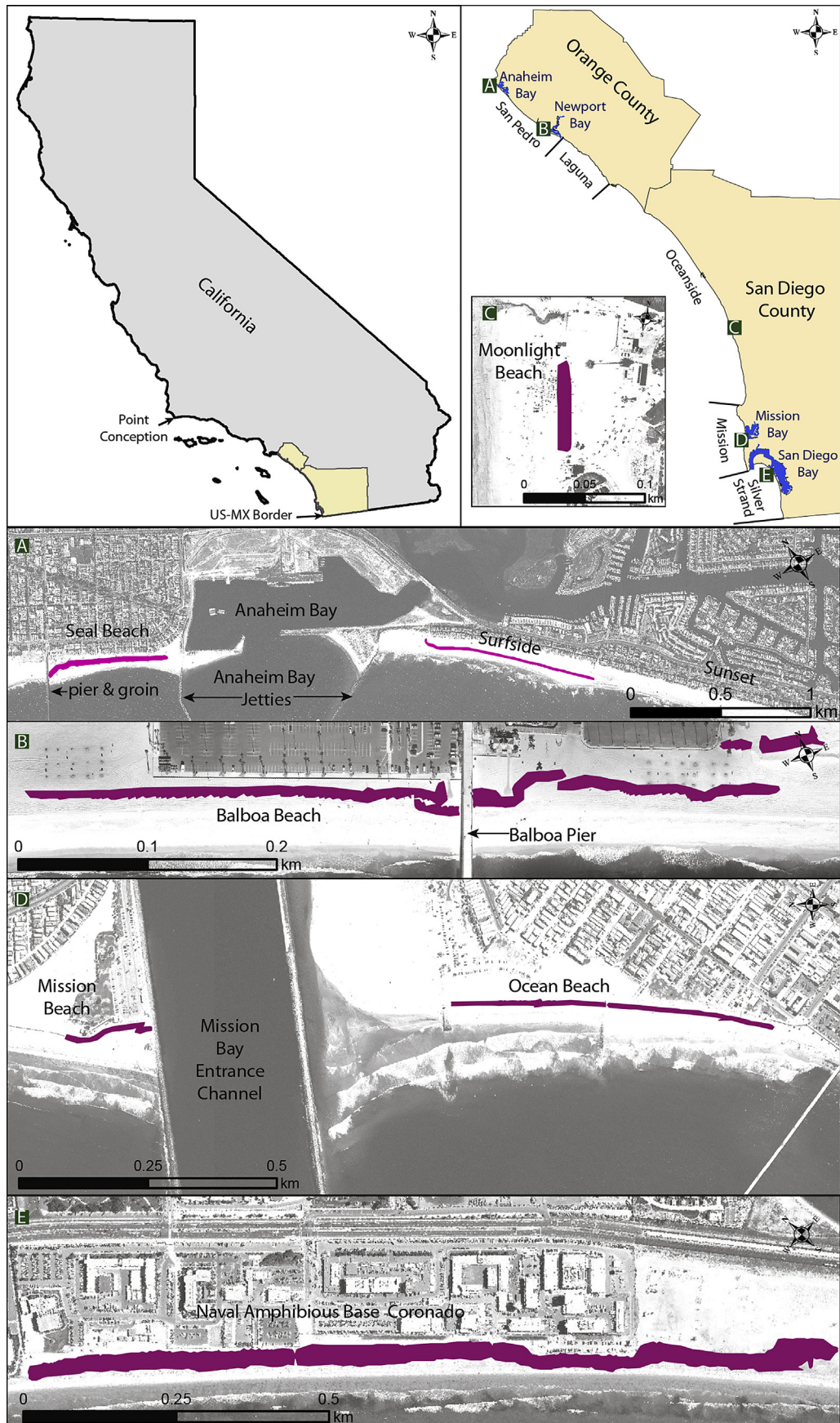
Fig. 2. General site locations are shown in the upper panels. Insets A-E show individual site extents and berm footprints (pink). (For interpretation of the references to colour in this figure legend, the reader is referred to the web version of this article.)

dike type structures protecting high value backshore infrastructure. Berm, wave, and water level observation methods are described in Section 2. Berm geometries are presented in Section 3 and compared with total water levels (contributions from waves and tides) in Section 4. Discussions of berm design (Section 5) and adaptation to higher water levels (Section 6) are followed by a summary (Section 7).

2. Methods

2.1. Site description

The southern California coast extends from Point Conception in Santa Barbara County to the US-Mexico border and represents the most urbanized stretch of coast in the state (Hapke et al., 2009). The bight is a microtidal environment, great diurnal range is ~1.6 m. Prevailing winter wave energy results from Pacific Northwest storms ($240° < D_p < 320°$) characterized by swell frequencies of 12–18 s and significant wave heights of over 2 m (Adams et al., 2008). Typical longshore transport is southward. Median grain diameters on southern California beaches range from ~0.13–0.50 mm (USACE, 2002). However, all beaches in this study have been nourished, larger grain sizes are reported (CSMW, 2013). Multiple beaches report berming (e.g., Malibu Times, 2005; Connelly, 2012; Carini, 2013) however, this study is restricted to Orange and San Diego Counties (Fig. 2), which are comprehensively covered in recurrent seasonal LiDAR observations from 2000 to 2009. The northern portion of Orange County is located within the San Pedro littoral cell extending from Point Fermin in Los Angeles County to Corona Del Mar, just south of Newport Bay. Three of the seven bermed beaches, Seal, Surfside and Balboa are within this area. Four San Diego County beaches, Moonlight Beach, Mission Beach, Ocean Beach and Coronado, located in the Oceanside, Mission and Silver Strand littoral cells respectively, show evidence of berming.

2.2. Geospatial data

Aerial LiDAR data was downloaded from NOAA digital Coast in NAD83 State Plane VI or VII (depending on location) and NAVD88 (NOAA, 2013). Regions containing sandy beach adjacent to urbanized backshore were individually examined in ArcMap (ESRI, Redlands, CA), and southern California newspapers were searched for articles referencing beach berms, artificial dunes and coastal flooding. Eleven possible berming sites were identified: Long Beach, Seal Beach, Sunset-Surfside, Newport Beach (Balboa), San Clemente, Moonlight Beach in Encinitas, Mission Beach, Pacific Beach, Ocean Beach, Naval Base Coronado (referred to hereafter as Coronado) and an area farther south in Silver Strand State Beach. Anthropogenic berms were found at eight sites, and analyzed at seven sites in Orange and San Diego Counties. Berm geometry was extracted from 34 of the 100 Lidar tiles reviewed.

2.3. Berm delineation

Berms were defined as dune-like structures on the back beach over 60 cm tall and exhibiting steep slopes relative to the ambient beach. Slopes between 7° and 45°, the maximum beach slope and maximum angle of repose of wet sand, respectively, correspond to anthropogenic dunes. Slopes steeper than ~45°, represent vegetation, vehicles and/or structures and were removed from analysis. Additionally, vegetated berms such as North Island in San Diego, and immediately south of the Naval Amphibious Base Coronado were also excluded from analysis. Individual berm cross-sections were examined to confirm both seaward and landward berm toes were appropriately delineated by the 7° steepness criterion (Fig. 3).

The elevation of berms ends ($Z_{\min}^{\mathrm{crest}}$), defined as the termination of high gradients using the same 7° threshold, are typically slightly above the ambient beach (~25 cm). Slopes within the target range were converted to polygons and artifacts from structures or gaps in the berm were manually removed or joined as needed. Moonlight Beach has a steep and continuous slope seaward of the berm, therefore the seaward toe was identified using the average elevation between the seaward berm ends.

2.4. Berm statistics

Berm geometries (area, volume, crest elevation and toe elevation) were estimated using ArcMap using a 2 m resolution digital elevation model (DEM). Length and crest elevation were determined along a crest line through the highest DEM pixels within the berm polygon. Toe elevation was determined by extracting DEM pixels along the seaward edge of the berm polygon. To calculate berm volume, a 3D reconstruction of the un-bermed beach was created using a triangular irregular network (TIN). The berm volume, V_{berm}, is defined as the volume above the reconstructed base (Figs. 5–11, dashed lines). The volume of sand above Mean Sea Level (MSL), V_{msl}, was calculated by subtracting the MSL plane from the surface DEM. MSL (in 1983–2001 epoch) was determined by the nearest tide gauge. Foreshore slope, β, defined here as the slope between the berm toe and mean lower low water (MLLW) was calculated in ArcMap.

2.5. Maximum water level and runup estimates

Total water level (TWL) is defined as the sum of tide gauge water levels and the 2% exceedance of wave runup estimated using Stockdon et al. (2006)

$$R_{2\%} = 1.1\left(0.35\beta(H_0 L_0)^{0.5} + \frac{\left[H_0 L_0\left(0.563\beta^2 + 0.004\right)\right]^{0.5}}{2}\right)$$

(1)

where H_0 is the deep water significant wave height. The deep water wave length, $L_0 = g/2\pi f_p^2$, is computed from the peak frequency, f_p. Water level was obtained from the nearest NOAA tide gauge in Los Angeles (9410660) or La Jolla (9410230) California (NOAA, 2013). Water levels are nearly identical between these two gauges (Flick, 1998; Schubert et al., in press), and when observations were unavailable the other gauge was substituted.

The CDIP buoy network (http://cdip.ucsd.edu) was used in combination with a spectral refraction model (O'Reilly and Guza, 1991, 1993, 1998) to estimate hourly significant wave heights along the 10 m depth contour (100 m alongshore spacing) seaward of each berm. The refraction model includes the effects of complex offshore (e.g., the Channel Islands) and local shelf bathymetry. Ocean swell predictions (here 0.04–0.1 Hz) are initialized with offshore buoy data and sea predictions (0.1–0.5 Hz) use nearby local deepwater buoys along the mainland shelf break. Incident wave energy and f_p were estimated as the mean of the alongshore 10 m depth predictions fronting the berm. The hindcast wave height in 10 m is linearly (un)shoaled to obtain H_0.

Comparison of modeled and observed waves at three buoys (not used in swell predictions) located near the bermed beaches show generally good prediction of wave energy E, but scatter in f_p (Fig. 4). Waves in southern California are often bimodal, with sea (nominally 0.2 Hz) and swell peaks (nominally 0.06 Hz) of comparable energy, and an observed f_p that jumps between sea and swell peaks. The wave model is not accurate enough to routinely reproduce the
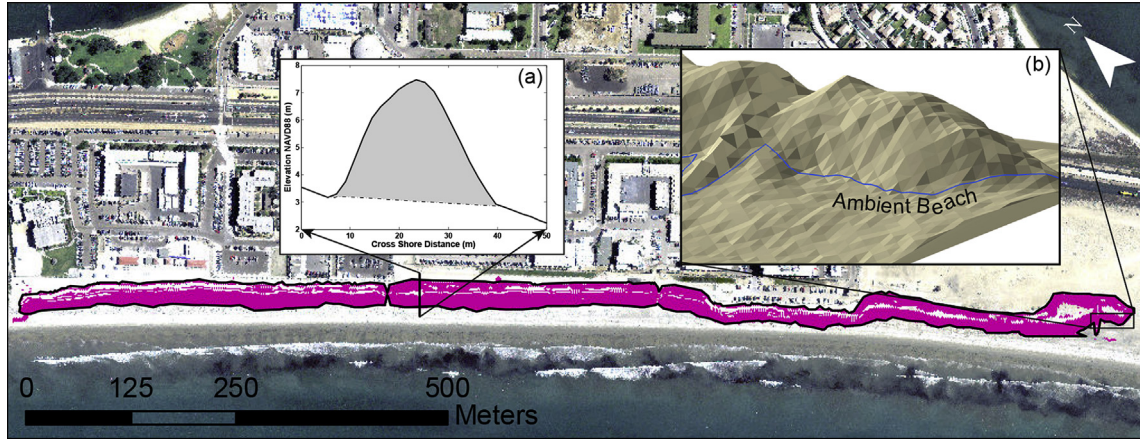
Fig. 3. Berm delineation methodology. Pink shows pixels with slopes of 7—45° and berm footprint outlined in black. Inset (a) berm cross-section (elevation versus cross-shore distance and estimated berm base). Inset (b) 3D berm end with berm footprint outlined in blue. (For interpretation of the references to colour in this figure legend, the reader is referred to the web version of this article.)
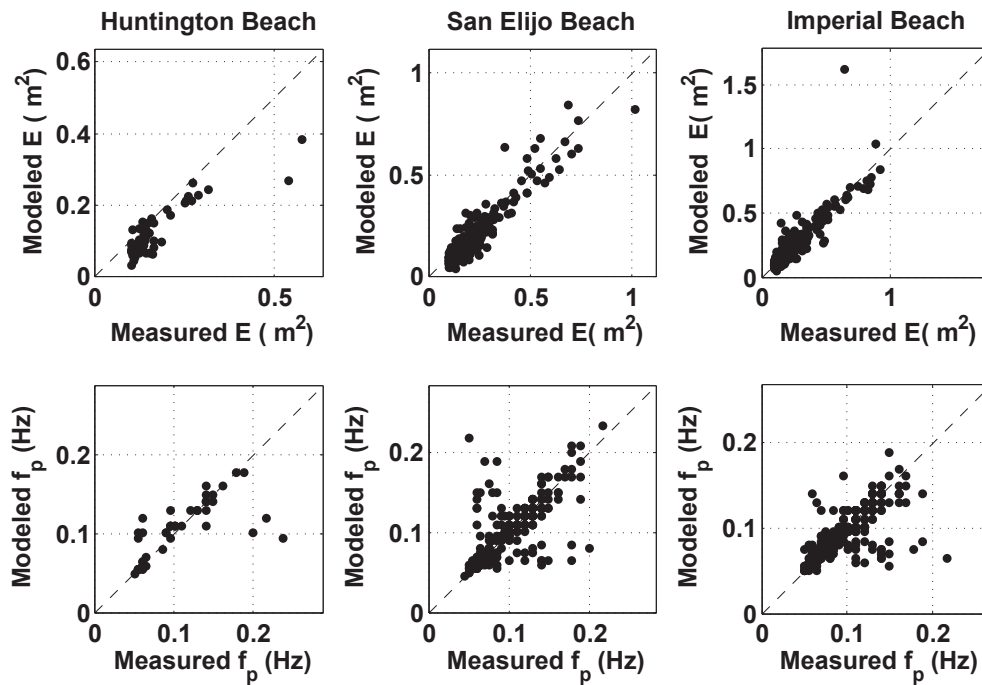

Fig. 4. Observed versus predicted wave energy E (top) and peak wave frequency f_p (bottom) at three buoys located near study berms. Each point corresponds to the 1 h record with the daily maxima of E, excluding cases with $E < 0.1$ m^2 (e.g., $H_s < 1.25$ m). Model validation periods are: Huntington State Beach (June 2005—November 2006), San Elijo State Beach (April 2009—July 2012), and Imperial Beach (December 2006—January 2010).

f_p instability in the observed data; however, the most extreme wave events are typically dominated by a single peak that is reproduced by the model. The widely used, Stockdon et al. (2006) empirical formula for runup (equation (1)) is based on field observations from many sources. In some cases, only the bulk properties of waves (e.g., wave height, peak period), were reported, so equation (1) is limited to those variables. $R_{2\%}$ depends strongly on f_p, and small changes in the relative sizes of sea and swell peaks can change f_p, producing large, non-physical differences in $R_{2\%}$. For example, with $H_0 = 3$ m and $\beta = 0.05$, for $f_p = 0.06$ and 0.2 Hz, $R_{2\%}$ is 2.2 and 0.65 m, respectively. The dependence of runup on wave spectral shape, omitted in equation (1), may be substantial, but is not well understood (Guza and Feddersen, 2012).

3. Berm geometry

Over 19 km of berms were identified at seven Orange County and San Diego beaches: Seal Beach, Sunset, Balboa Beach, Moonlight Beach, Mission Beach, Pacific Beach, Ocean Beach and Coronado. Beach volumes and berm geometries are summarized in Tables 1 and 2. Although pre-2000 data was included for beach volume calculations, LiDAR data in 1997 and 1998 was incomplete, so berm statistics are calculated post-2000. The berms separate into three characteristic categories based on deployment duration: event, seasonal and persistent.
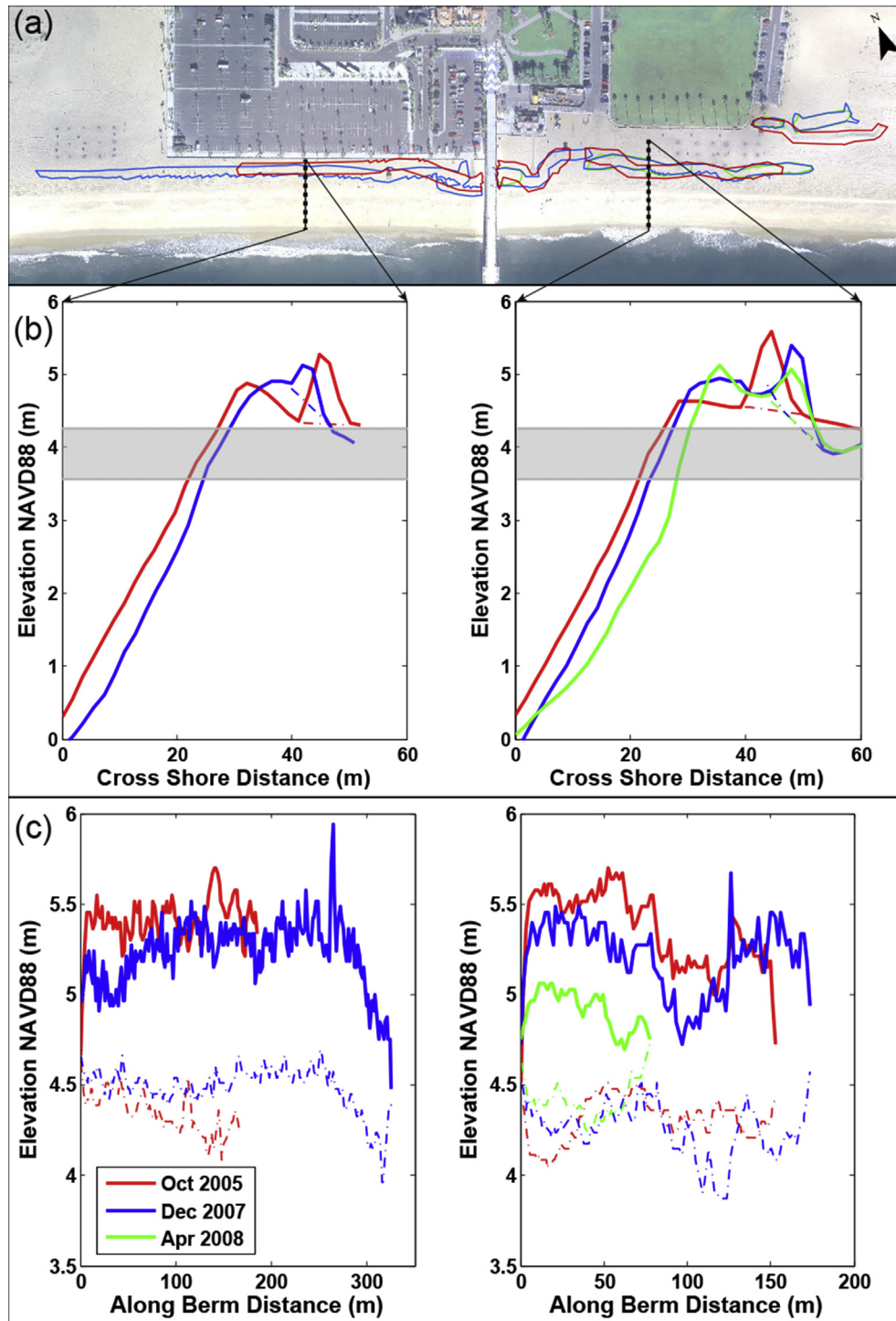
Fig. 5. Balboa Beach berms: (a) plan view with footprints outlined in color, (b) berm cross-sections (solid) along transects and estimated berm bases (dashed). The gray bands show the range of maximum TWLs for high runup events. (c) Crest (solid curves) and base elevations (dashed curves) versus along-berm distance. Colors correspond to dates (see legend). (For interpretation of the references to colour in this figure legend, the reader is referred to the web version of this article.)

3.1. Event berms

Temporary berms are deployed at Balboa Beach, Mission Beach and Ocean Beach on an as-needed basis for anticipated high water level events. Event berms share three common features: triangular cross section, low berm to beach volumes (~2%) and crest elevations of ~5 m.

3.1.1. Balboa beach

The wide beach at Newport typically infiltrates any overtopped water, however the areas adjacent to Balboa Pier are paved public parking lots which serve to collect and transfer overtopping volumes to the substantially lower urbanized backshore (Gallien et al., 2014). Temporary berms are constructed by the City of Newport Beach in anticipation of runup and overtopping, though small reaches adjacent to the pier are bermed semi-permanently. Balboa
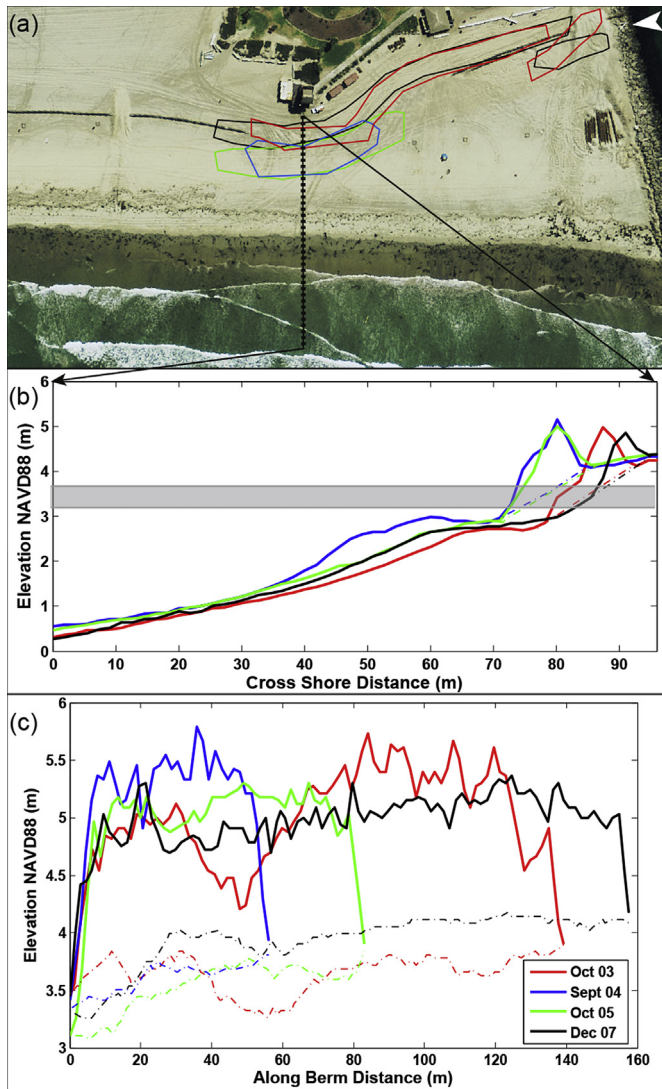
Fig. 6. Mission Beach berms: (a) plan view with footprints outlined in color, (b) berm cross-section (solid) along transect and estimated berm base (dashed). The gray bands show the range of maximum TWLs for high runup events. (c) Crest (solid curves) and base elevations (dashed curves) versus along-berm distance. Colors correspond to dates (see legend). (For interpretation of the references to colour in this figure legend, the reader is referred to the web version of this article.)

berms (Figs. 1a and 5) are scraped from either the fore- or back-shore and consist of a series of small, often discontinuous berms spanning an average length of 469 m. Balboa Beach has the highest volume relative to MSL, $V_{msl} = 300$ m³/m. The berm volume, V_{berm}, is 4 m³/m. The beach crest elevation ~5 m is the highest on a cross-peninsula transect. Balboa has the steepest foreshore slope (*ca.* 1:10) in the study.

3.1.2. Mission beach
Mission Beach is a highly urbanized sand spit backed by Mission Bay to the east, a small berm (Fig. 6) is constructed by the City of San Diego Parks and Recreation Department. The entirety of Mission Beach is protected by a concrete sea wall (CDBW, 1994). Mission Beach is highly vulnerable to flooding, and in the 1982-1983 and 1997–1998 El Niños the sea wall was overtopped (CDBW, 1994). The berm is built on an unusually wide beach near the jetty, consequently the average beach volume, 276 m³/m, is significantly higher than is typical of the area. At Mission Beach, $V_{berm} = 8$ m³/m,

approximately 2% of V_{msl}. The berm crest elevation is 4.97 m, the berm is 127 m long, and the foreshore slopes are shallow, about 1:30.

3.1.3. Ocean beach
Ocean Beach is located immediately south of Mission Beach and separated by the Mission Bay entrance channel (Figs. 2D and 7). Ocean Beach is a pocket beach, approximately 1 km long with an average beach volume of 173 m³ backed by dense residential and commercial property. The small berm, $V_{berm} = 4$ m³/m (Fig. 7), is constructed as needed by the city of San Diego Parks and Recreation Department. A significant Ocean Beach berm, over 2000 m long, present only in the December 2007 survey, has three distinct sections with an average crest elevation of ~4.5 m. A much shorter 268 m long berm present in October 2003 was included in average toe, crest elevation, toe elevation and beach slopes, but excluded from the average length calculation.

3.2. Seasonal berms

Seasonal berms are deployed at Seal Beach, Surfside and Moonlight Beach to mitigate winter storm flooding. They exhibit higher crest and toe elevations, and larger relative volumes V_{berm}/V_{msl} ~ (5–10%), than event berms.
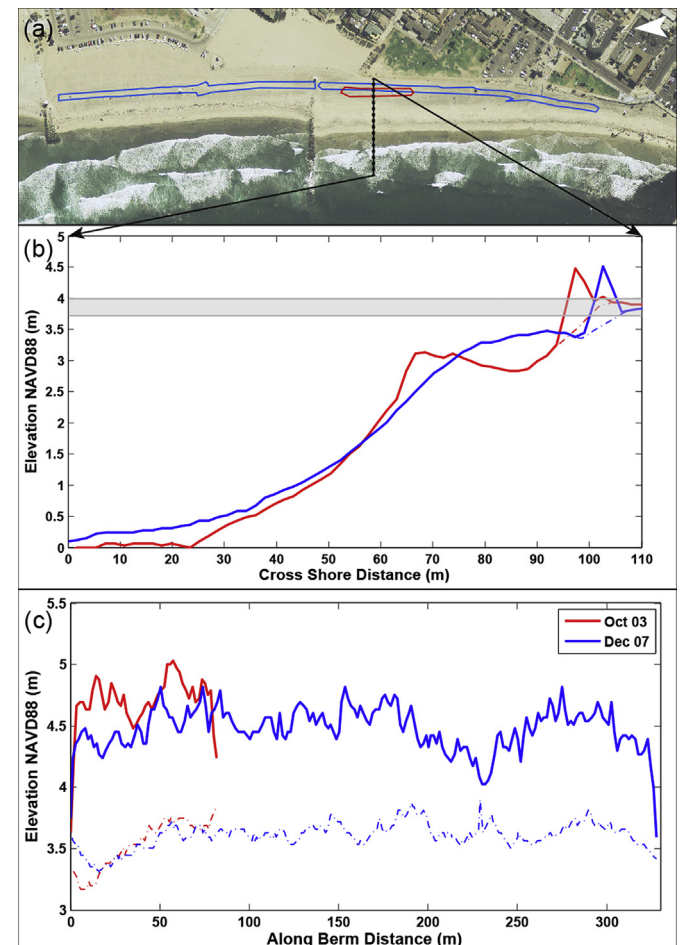

Fig. 7. Ocean Beach berms: (a) footprints, (b) cross-sections, (c) along-berm crest and base elevations. (See Fig. 6 caption for details.) The low elevation passage in December 2007, where the footprint is discontinuous (a), was fronted by a low elevation (<60 cm) berm (not shown) that deflected runup from the passage.
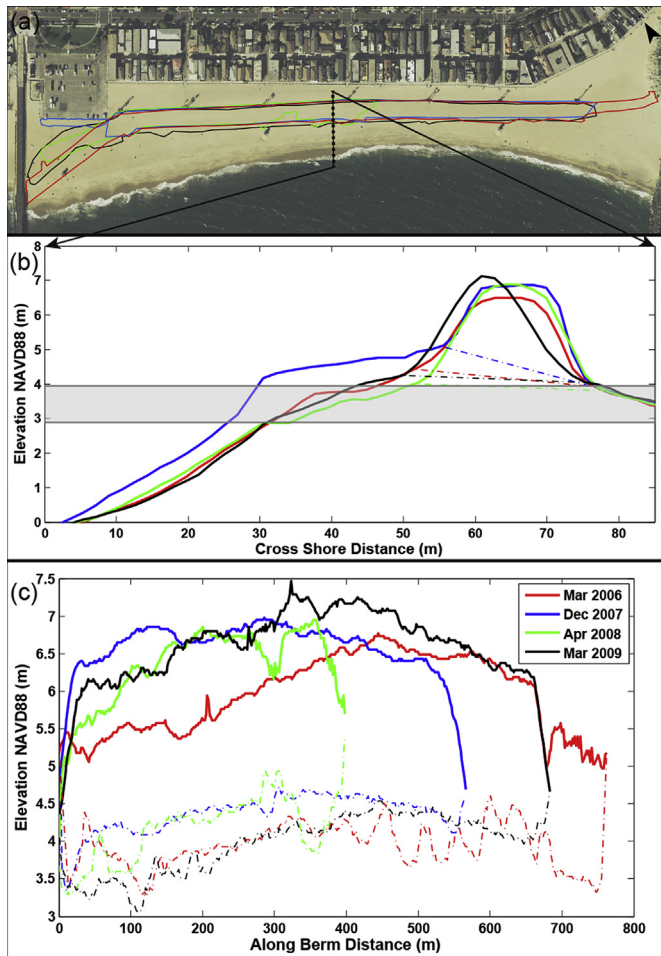
Fig. 8. Seal Beach berms: (a) footprints, (b) cross-sections, (c) along-berm crest and base elevations. (See Fig. 6 caption for details.)
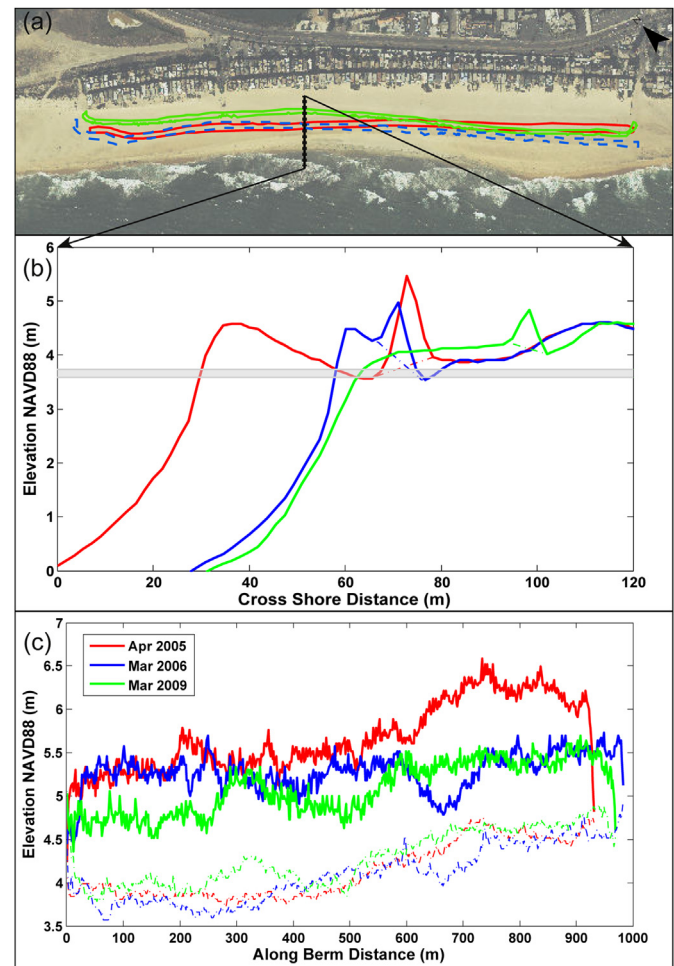

Fig. 9. Surfside Beach berms: (a) footprints, (b) cross-sections, (c) along-berm crest and base elevations. (See Fig. 6 caption for details.)

3.2.1. Seal beach

Seal Beach is the largest seasonal berm (Fig. 8), approximately 28 m^3/m (V_{berm}) and 620 m long. In April 2008 the berm is less than 400 m long, it appears the eastern section of the berm was razed prior to the LiDAR survey. This berm is built from relocated west beach sand (sand backpassing) or in some cases, opportunistic nourishment from dredging projects. The berm is designed to protect a very low backshore (<4 m NAVD88) and has been erected annually for decades in October or November and typically removed by mid-March. The average observed berm crest elevation is 6.3 m NAVD88. The engineered crest elevation is quoted at 5.5 m (City of Seal Beach (2010)), and although no datum reference is given the average observed berm crest elevation is consistent with a berm 5.5 m above MSL. The wide, nearly flat crest approximates a rectangular cross-section. Typically, the berm is continuous. How-ever, in December 2007 the main berm (with the typical rectan-gular cross-section, spanning over 500 m with 6.5 m elevation) was accompanied by a small triangular shaped western berm (~77 m length with average ~5 m elevation). Public documents quote the cost of berm building at $70,000 in 2008—2009 and $131,600 in fiscal year 2009—2010. The cost difference is likely the backpassing of sand from west to east beach required every other year (City of Seal Beach 2009; 2010).

3.2.2. Surfside

Surfside, the community immediately southwest of Seal Beach, is a sand spit backed by Anaheim Bay (Fig. 9). Surfside suffers chronic erosion and has received multiple nourishments and a 580 m revetment (USACE, 2002). A long (ca. 1 km), but small, V_{berm} ~ 6 m^3/m and ~5 m crest elevation, berm is erected annually in November or December and regraded in March or April to protect approximately 280 homes (Surfside, 2012). Surfside is the lowest volume study beach (V_{msl} ~ 100 m^3/m) and second steepest fore-shore slope ~ 1:13.

3.2.3. Moonlight

Moonlight Beach, shown in Fig. 10, is a small (~150 m long), heavily used pocket beach formed in the floodplain of a small creek. The beach is backed by park facilities vulnerable to flooding and damage (Armstrong and Flick, 1989; CDBW, 1994). Berms are typically erected in October and graded in April (City of Encinitas, 2007). A combination of native sand scraped from above mean higher high water (MHHW) and imported sand are used to com-plete the berm (City of Encinitas, 2007). The berm volume is ~8 m^3/m, approximately average. The Moonlight berm is the shortest (70 m) of all study berms. Average crest elevation is ~6.4 m and mean foreshore beach slope is ~1:16.
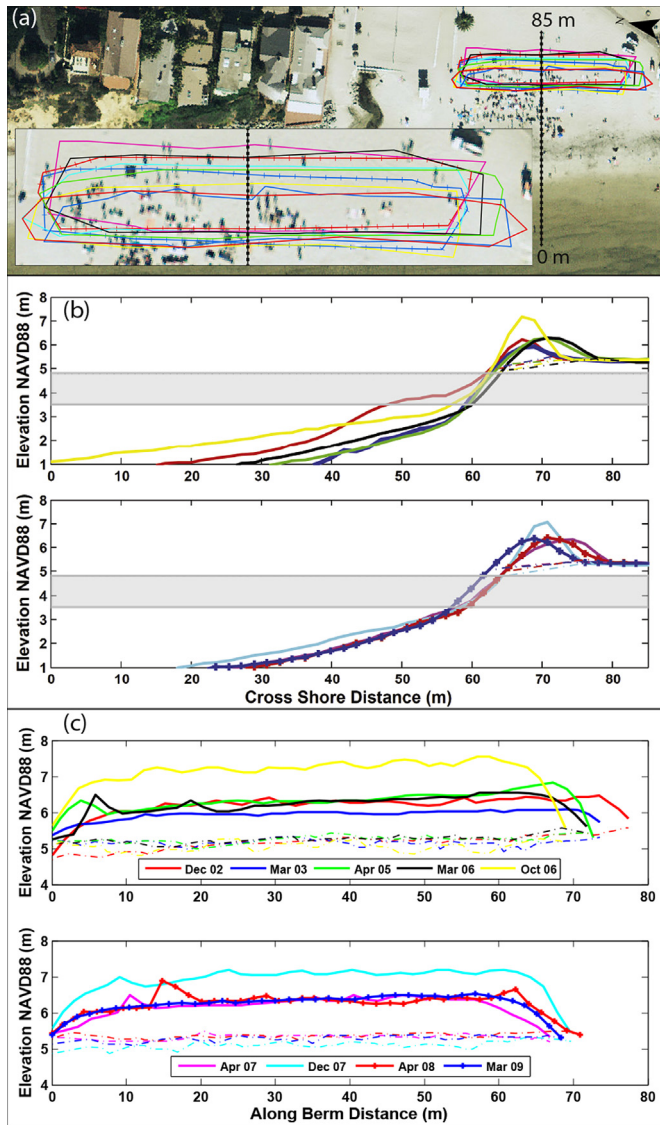
Fig. 10. Moonlight Beach berms: (a) footprints, (b) cross-sections, (c) along-berm crest and base elevations. (See Fig. 6 caption for details.)

3.3. Persistent: Coronado

Coronado Beach is located on a wide barrier spit separating the Pacific Ocean and San Diego Bay. The site received over 28,000,000 m³ of nourishment from San Diego Bay dredging projects and a large berm was built to protect Naval Amphibious Base Coronado (CDBW, 1994). The Coronado berm (Fig. 11) is the largest of the study, 48 m³/m, representing almost one quarter of the total beach volume above MSL. Additionally, it is the longest (~1.3 km) and highest (6.77 m) of all study berms. The berm appears in all LiDAR data sets of the area, and is periodically reshaped. The berm protects a low backshore (<3.5 m), and has multiple discontinuities (likely vehicle passages). The foreshore slope is the mildest of the study, ~1:34.

4. Water levels and berms

The maximum observed water level at the Los Angeles and La Jolla tide gauges was ~2.2 m NAVD88. Waves add an additional 1–3 m and maximum total water levels ranged from 3.1 to 4.8 m

NAVD88, exceeding the ~4 m beach and backshore elevations at Balboa Beach, Ocean Beach, Seal Beach and Coronado. Table 3 shows the individual maximum total water levels in comparison to berm elevations.

Overwash and slumping from undercutting or notching are primary dune failure methods (Judge et al., 2003). Flow around the berm ends (Fig. 1a, inset) represents an additional failure mode observed in anthropogenic flood control berms. Overtopping is defined to occur when the runup of individual waves exceeds the berm crest elevation (i.e., $R_{2\%} > Z_{avg}^{crest}$). End flow is controlled by wave runup relative to the crest elevation (Z_{min}^{crest}) as it converges toward the un-bermed beach surface (Fig. 3b). Berm avalanching (i.e., slumping or notching) is the cumulative effect of water level and waves interacting with the berm toe (Z_{min}^{toe}). Failure modes may occur concurrently.

Southern California berms interact with coincident high water levels and energetic waves only a few hours during a given deployment. In no case did maximum water levels, shown as the gray bands in Figs. 5–11, exceed crest elevations, suggesting
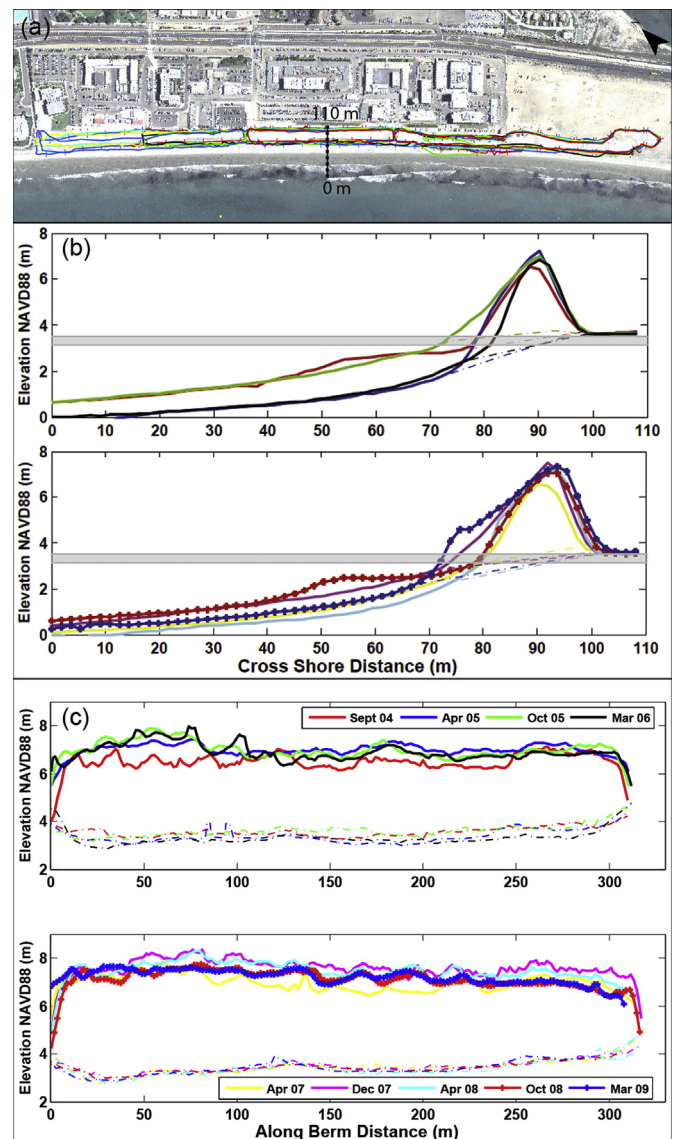

Fig. 11. Coronado Beach berms: (a) footprints, (b) cross-sections, (c) along-berm crest and base elevations. (See Fig. 6 caption for details.)

Table 1
LiDAR availability and beach volumes above MSL, all units are in m³/m. (−) indicates LiDAR data was unavailable, (*) indicates poor LiDAR resolution prevented calculation. The standard deviation of beach volume is δ.

Year	Month	Seal	Surfside	Balboa	Moonlight	Mission	Ocean	Coronado
2009	Mar	272	81	302	156	283	*	179
2008	Oct	263	88	312	197	295	177	193
2008	Apr	273	76	282	154	264	163	153
2007	Dec	283	95	297	172	302	176	194
2007	Apr	237	82	283	152	263	162	161
2006	Oct	253	104	314	207	–	–	–
2006	Mar	260	89	304	150	257	163	143
2005	Oct	247	122	312	173	313	182	208
2005	Apr	235	112	293	141	274	192	172
2004	Sep	244	128	–	188	318	188	196
2004	Apr	–	–	–	–	–	–	–
2003	Oct	–	–	317	157	282	*	–
2003	Mar	–	–	–	135	–	–	–
2002	Dec	–	–	–	184	–	–	–
2002	Sep	–	–	–	208	–	–	–
2002	May	–	–	–	187	–	–	–
1998	Spr	244	73	280	130	189	*	147
1997	Fall	*	*	*	*	*	*	*
Mean	All	255	96	300	168	276	173	178
δ	All	15.7	18.6	13.7	24.9	35.4	10.8	21.9

Table 2
Summary Statistics for all berms present in 2000–2009 LiDAR data. Standard deviation in shown in parentheses. All units are in m unless otherwise noted.

Beach	Berm type	$\bar{L}$	$\bar{V}(m^3/m)$	Z_{crest}	Z_{toe}	β	Vol (%)
Balboa	Event	469(240)	4(2)	5.02(0.27)	4.61(0.21)	9.48	1.5
Mission	Event	127(67)	7(3)	4.97(0.11)	3.22(0.31)	29.44	2.5
Ocean	Event	–	4(1)	4.59(0.26)	3.27(0.11)	20.23	2.2
Seal	Seasonal	621(157)	28(1)	6.30(0.24)	4.50(0.46)	14.19	10.2
Surfside	Seasonal	961(312)	6(3)	5.32(0.29)	4.39(0.15)	12.84	4.9
Moonlight	Seasonal	71(3)	8(3)	6.37(0.40)	5.29(0.11)	15.95	4.8
Coronado	Persistent	1218(161)	48(7)	6.77(0.25)	2.86(0.29)	33.64	27.4

overtopping did not occur. Five individual berms were at risk of end flow (i.e., $R_{2\%} > Z_{min}^{crest}$) on up to ten occasions (Table 4); Newport Beach in 2008 and 2005, Mission Beach in 2007 or 2005 and Ocean Beach in December 2007 (the highest level of end flow, Fig. 7). Note that all end flow event waves are relatively long period (14 + sec), highlighting the strong dependency of $R_{2\%}$ (equation (1)) on $L_o \sim 1/f_p^2 \sim T_p^2$. The minimum crest elevation, Z_{min}^{crest}, is slightly higher than the ambient beach elevation, but only 2% of runups reach this level and the volume of end flow associated with an event is unknown.

Total water level (TWL) exceeded the toe elevation of most berms, allowing at least limited avalanching. Note that at Coronado the slope break occurs near MHHW suggesting the seaward toe is under consistent attack. However, the percentage of berm volume under attack relative to the total seaward berm volume is small (~2%). A significant avalanching event is defined here as a minimum of 10% of the seaward berm volume exposed to the total water level for one of more hours (Table 5). The event berms at Balboa Beach and both Ocean Beach berms were subject to significant avalanching conditions. The December 2007 berm at Ocean Beach stands out as a particularly vulnerable, both end flow and avalanching may have occurred.

LiDAR flights and coincident high TWL are rare. Only four berms at Balboa, Mission and Ocean beaches were surveyed shortly before or after high water events. The October 2005 flight (Table 4) captured berms at Balboa and Mission Beach that were likely prepared for the September 16, 2005 high tide (1.86 m) and long period swell ($T_p \sim 20$ s). Similarly, the December 2007 LiDAR data, flown in late November (Table 4), captures the berms at Ocean and Mission Beach present for the December 5, 2007 energetic wave event ($H_s \sim 3$ m, $T_p \sim 18$ s). Maximum TWL and minimum berm elevations differed by less than 15 cm for three of these events,

suggest near optimal berm design. The berms were sufficiently high to prevent overtopping, but no taller than necessary.

5. Berm monitoring and design

Monitoring the performance of these widely used, but not well understood, mitigation structures is critical to assessing future adaptation strategies for the urban coast. Figlus et al. (2011) suggests berm resiliency depends on berm geometry and although literature mentions temporary anthropogenic sand dunes for flood control, location, geometrical properties or performance of these critical structures are not widely addressed and represents a significant gap in the current literature.

The highest total water levels and potential berm failures are caused by a combination of high tides and energetic long period swell (Tables 4 and 5). The maximum duration event was 4 h and most events were 1–2 h. Stockdon $R_{2\%}$ runup represents the maximum elevation of the runup tongue which carries only nominal volume. From a flood modeling perspective, the volume of water that overtops the berm or flows around the ends is the fundamental quantity of interest, thus berm efficacy hinges on the maximum admitted volume. Optimization of berm design requires careful consideration of the berm length, placement, beach width (infiltration) and end flow conditions. Designs may be optimized using maximum allowable volume for overtopping and end flow instead of runup alone. Unfortunately, empirical overtopping models do not accurately estimate overtopping rates (Laudier et al., 2011; Gallien et al., 2014) and numerical overtopping models are insufficiently validated in the field.

Currently berms actively deflect high TWL events for only a few hours per year and erosion of these berms is minimal. The

Table 3
Observed Water Levels (OWL), total water level, crest elevations, toe elevations and hours exceeding given crest and toe elevations. All units are in meters NAVD88.

Beach	Yr	Mo	OWL_{max}	TWL	Z_{avg}^{crest}	Z_{min}^{crest}	Z_{avg}^{toe}	Z_{min}^{toe}	$V(m^3/m)$	$hr > Z_{min}^{crest}$	$hr > Z_{min}^{toe}$
Seal	2009	Mar	2.20	3.46	6.54	4.36	4.08	2.85	28	0	104
	2008	Apr	2.22	3.67	6.32	3.81	4.72	3.29	28	0	8
	2007	Dec[a]	2.09	3.95	6.38	4.64	5.05	3.87	28	0(3)[a]	2(326)[a]
	2006	Mar	2.10	2.88	5.97	4.84	4.17	2.79	26	0	7
Surfside	2009	Mar	2.20	3.67	5.07	4.18	4.50	3.94	3	0	0
	2006	Mar	2.10	3.73	5.26	4.21	4.46	3.86	5	0	0
	2005	Apr	2.32	3.58	5.64	4.14	4.22	3.54	8	0	3
Balboa	2008	Apr	2.22	4.25	4.75	4.06	4.41	3.46	3	2	163
	2007	Dec	2.09	3.55	4.96	3.87	4.68	3.12	4	0	86
	2005	Oct	2.32	3.86	5.31	3.80	4.37	3.28	6	3	145
Moonlight	2009	Mar	2.19	3.73	6.23	5.08	5.34	4.90	7	0	0
	2008	Apr	2.19	4.78	6.23	5.31	5.12	4.70	7	0	1
	2007	Dec	2.09	4.40	6.94	5.31	5.44	4.73	12	0	0
	2007	Apr	2.09	4.37	6.20	5.36	5.46	5.04	8	0	0
	2006	Oct	2.10	3.50	7.13	5.64	5.21	4.41	12	0	0
	2006	Mar	2.10	3.68	6.18	4.90	5.27	4.76	8	0	0
	2005	Apr	2.27	4.28	6.29	5.33	5.32	4.93	8	0	0
	2003	Mar	2.15	4.45	5.92	5.43	5.20	4.51	5	0	0
	2002	Dec	2.10	3.89	6.18	4.97	5.23	4.51	5	0	0
Mission	2007	Dec	2.09	3.67	5.74	3.54	3.68	2.93	4	2	28
	2005	Oct	2.27	3.55	5.41	3.12	3.04	2.80	9	17	129
	2004	Sep	2.18	3.26	5.90	3.40	3.01	2.76	11	0	127
	2003	Oct	2.15	3.20	5.78	3.35	3.34	2.70	6	0	134
Ocean	2007	Dec	2.09	4.00	4.41	3.61	3.34	2.89	4	5	165
	2003	Oct	2.15	3.73	4.78	4.03	3.19	2.65	5	0	544
Coronado	2009	Mar	2.19	3.14	6.84	4.49	2.72	1.89	61	0	1654
	2008	Oct	2.19	3.32	6.89	4.01	2.99	1.97	50	0	1302
	2008	Apr	2.19	3.53	6.98	3.65	2.54	1.52	52	0	4111
	2007	Dec	2.09	3.40	7.13	3.52	2.94	2.28	52	0	391
	2007	Apr	2.09	3.42	6.61	3.69	2.76	2.10	45	0	836
	2006	Mar	2.10	3.15	6.74	3.54	2.50	1.51	46	0	4512
	2005	Oct	2.27	3.16	6.48	3.42	3.34	2.04	40	0	1228
	2005	Apr	2.27	3.25	6.93	4.40	2.73	1.73	48	0	2880
	2004	Sep	2.18	3.20	6.36	4.17	3.25	1.41	36	0	4846

[a] Elevations are given for the main berm (Fig. 8). Exceedance hours including the small western berm are in parentheses.

2000–2009 data did not include a significant El Niño event, however higher future TWLs associated with sea level rise or El Niño greatly increase the number of impact hours per year (Fig. 12). As berm duty cycles increase, morphological feedback and failure mechanisms become critical to flood forecasting. A berm can be completely eroded by wave attack without runup ever reaching the original (uneroded) crest level.

6. Alternative scenarios and adaptation

If an additional 30 cm of water level, consistent with a strong El Niño, were considered, nearly all event berms would experience end flow, and impact hours increase dramatically to over 27 h per berm per year. Event berm end flow exposure increases from <1 h/berm/year to 5 h/berm/year (Fig. 12a) while Coronado's exposure increases from nearly zero to 1 h/berm/yr. From an avalanching perspective, only the event berms become vulnerable with a 30 cm

increase in TWL. If an additional 93 cm, the average of estimates for the Los Angeles region in 2100 (National Research Council, 2012) is considered, two event berms crests are overtopped and nearly all berms experience end flow. Additionally, the persistent berm at Coronado becomes vulnerable to avalanching.

Currently, berms are located on or near the highest portion of the beach Landward migration is limited by significant development. Elevating the berm crest alone would likely not provide sufficient protection, because berms subjected to chronic interaction are vulnerable to rapid avalanching and deterioration (Schubert et al., in press). Nourishment may be required to maintain present levels of protection. For illustrative purposes, we assume the entire profile shoreward of MSL is elevated by the same amount. For 25, 60, 110 and 170 cm of water level rise, approximately 10%, 25%, 50% and 100% increase in volume above MSL is required, respectively (Fig. 12b). In the near term, 30 cm of SLR requires nourishments ranging 13,300 m³ for short reaches such as Moonlight Beach to over 238,000 m³ at longer reaches. Longer term, extensive nourishments (~400,000 m³) may be required. However, nourishment plans must be carefully considered, recent evidence suggests nourishment sand may, in some cases, increase flooding of homes (Moreno, 2013). Finally, the steepest portions of the beach are directly in front of the berm, sustained higher water

Table 4
Potential end flow events.

Beach	LiDAR	Date	#hr	Tide(m)	$H_s(m)$	$T_p(s)$	$WL_{max}(m)$	Z_{min}^{crest}
Balboa	Apr 2008	7-31-08	2	1.98	0.94	16.7	4.25	4.06
	Oct 2005	9-16-05	2	1.86	0.64	20.0	3.86	3.80
Mission	Dec 2007	12-05-07	2	1.54	3.03	18.2	3.67	3.54
	Oct 2005	9-16-05	1	1.86	0.98	20.0	3.14	3.12
		12-21-05	2	1.15	3.25	18.2	3.26	3.12
		12-28-05	1	1.37	2.13	20.0	3.23	3.12
		12-29-05	3	1.82	1.91	18.2	3.44	3.12
		12-30-05	3	1.96	1.66	15.0	3.21	3.12
		12-31-05	1	2.04	1.41	14.7	3.17	3.12
Ocean	Dec 2007	12-05-07	4	1.66	3.01	18.2	4.01	3.61

Table 5
Significant avalanching events.

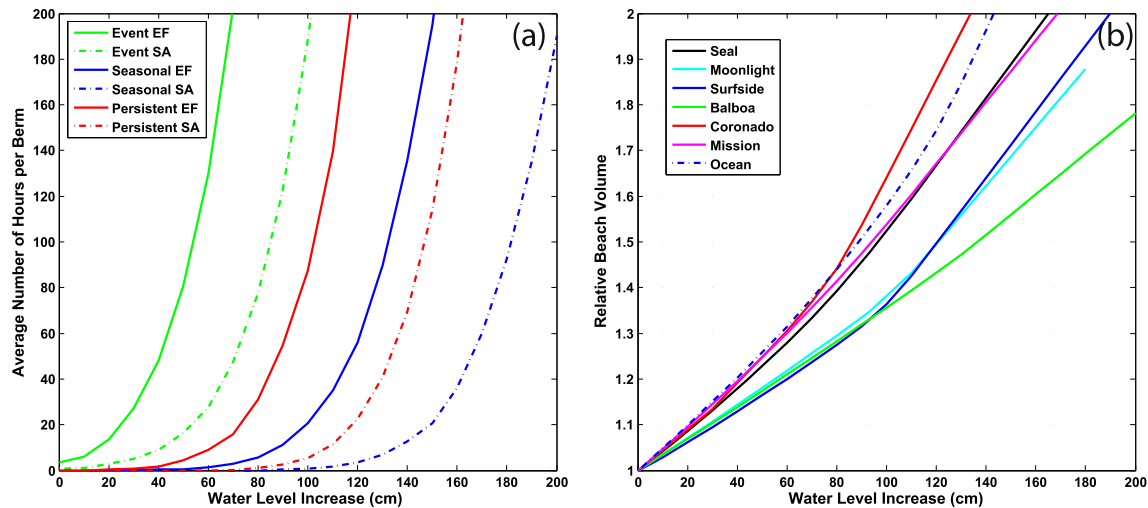| Beach	LiDAR	Date	#hr	Tide(m)	$H_s(m)$	$T_p(s)$	$WL_{max}(m)$	$Z_{10\%}$
Balboa	Apr 2008	7-31-08	1	2.15	0.94	16.7	4.25	4.22
Ocean	Dec 2007	12-05-07	4	1.66	3.01	18.2	4.01	3.67
	Oct 2003	3-16-03	1	1.69	3.27	14.7	3.73	3.68

Fig. 12. Water level increase impacts on (a) average number of exceedance hours per berm and (b) required relative beach volumes to maintain current levels of protection. End flow (EF, solid curve) and significant avalanching (SA, dashed curve) vulnerabilities are shown.

levels may interact with a steeper foreshore and consequently increase runup and therefore end flow and overtopping volumes.

7. Conclusions

The volumes and geometries of 34 berms in southern California are characterized using 18 LiDAR datasets spanning nine years. Three berm classifications emerged based on deployment duration: event, seasonal and persistent. Event berms are temporary structures with triangular cross-sections, relatively low volumes (~4 m^3/m) and crest elevations (~5 m NAVD88). Seasonal berm are larger, volumes vary from 6 to 28 m^3/m, and average crest elevations between 5.3 and 6.4 m. One persistent berm, captured in all LiDAR data for that area, is the largest (48 m^3/m), longest (1.2 km), and highest mean crest elevation (7 m) of all study berms. Total water levels, estimated using observed tides and a regional wave model coupled with an empirical runup formula, suggest that overtopping is rare. Concerningly however, berms may fail through avalanching associated with berm toe and water level interaction without TWLs ever reaching the initial berm crest elevation.

Anthropogenic berms protect numerous urbanized coastal reaches of southern California from flooding by coincident high water levels (~MHHW) and long period swell (14 + seconds). Currently, berms are active for relatively short durations (1–4 h), modest sea level rise (~25 cm) or higher water levels associated with El Niño, will increase exposure significantly and substantial nourishments may be required to maintain current levels of flood protection. Comprehensive future monitoring of anthropogenic flood mitigation berms is crucial to developing berm deployment guidance, optimizing future designs and accurate coastal hazard prediction.

Acknowledgments

References

Adams, P.N., Inman, D.L., Graham, N.E., 2008. Southern California deep-water wave climate: characterization and application to coastal processes. J. Coast. Res. 24 (4), 1022–1035.

Airoldi, L., Abbiati, M., Beck, M.W., Hawkins, S.J., Jonsson, P.R., Martin, D., Moschella, P.S., Sundelöf, A., Thompson, R.C., Åberg, P., 2005. An ecological perspective on the deployment and design of low-crested and other hard coastal defence structures. Coast. Eng. 52, 1073–1087.

Armstrong, G.A., Flick, R.E., 1989. Storm damage assessment for the January 1988 storm along the southern California Shoreline. Shore Beach 57 (4), 18–23.

Bochev-van der Burgh, L.M., Wijnberg, K.M., Hulscher, S.J.M.H., 2011. Decadal-scale morphologic variability of managed coastal dunes. Coast. Eng. 58, 927–936.

Brock, J., Wright, C., Sallenger, A., Krabill, W., Swift, R., 2002. Basis and methods of NASA airborne topographic mapper lidar surveys for coastal studies. J. Coast. Res. 18, 113.

Bruun, P., 1983. Beach scraping – is it damaging to beach stability? Coast. Eng 7, 167–173.

California Department of Boating and Waterways (CDBW), 1994. Shoreline Erosion Assessment and Atlas of the San Diego Region Volume II (Sacramento, California).

Carini, D., February 15, 2013. Venice Beach Sand Dunes Removed for the Season. In: Venice Patch. Available online at: http://venice.patch.com/groups/editors-picks/p/venice-beach-sand-dunes-removed-for-the-season.

Carley, J.T., Shand, T.D., Coghlan, I.R., Blacka, M.J., Cox, R.J., Littman, A., Fitzgibbon, B., McLean, G., Watson, P., 2010. Beach Scraping as a Coastal Management Option, 19th NSW Coastal Conference, Batemans Bay, NSW. Available at: http://coastalconference.com/2010/papers2010/JamesCarleyfullpaper.pdf.

Casas, A., Riaño, D., Greenberg, J., Ustin, S., 2012. Assessing levee stability with geometric parameters derived from airborne LiDAR. Remote Sens. Environ. 117, 281–288.

City of Encinitas Community Development Department, 2007. Notice of Decision PBD-2007-51, p. 6. Available at: http://archive.ci.encinitas.ca.us/weblink8/DocView.aspx?id=635687.

City of Seal Beach, June 30, 2009. Comprehensive Annual Financial Report for the Year Ended, p. 156. Available at: http://www.sealbeachca.gov/uploadedFiles/ComprehensiveAnnualFinancialReport2008-09.pdf.

City of Seal Beach, June 30, 2010. Comprehensive Annual Financial Report for the Year Ended, p. 153. Available at: http://www.sealbeachca.gov/uploadedFiles/ComprehensiveAnnualFinancialReport2009-10.pdf.

Clark, R., 2005. Hurricane Dennis Supplemental Damage Assessment Report: Impact of Hurricane Dennis on Dog Island and Discussion of Post-Storm Recovery Responses. Florida Department of Environmental Protection, Division of Water Resource Management, Bureau of Beaches and Coastal Systems.

Coastal Sediment Management Workgroup (CSMW), 2013. Beach Nourishment Projects in California. California Department of Boating and Waterways, Sacramento, California. Available online at: http://dbw.ca.gov/csmw/PDF/TABLE2TASK3CSMW.pdf.

Connelly, L., November 27, 2012. Seal Beach officials Prepare for High Surf. In: Orange County Register. Available at: http://www.ocregister.com/articles/beach-378901-swell-sand.html.

Cooke, B.C., Jones, A.R., Goodwin, I.D., Bishop, M.J., 2012. Nourishment practices on Australian sandy beaches: a review. J. Environ. Manag. 113, 319–327.

Cooper, J.A.G., Lemckert, C., 2012. Extreme sea-level ride and adaptation options for coastal resort cities: a qualitative assessment from the Gold Coast of Australia. Ocean Coast. Manag. 64, 1–14.

Dean, R.G., 2001. Beach Nourishment Theory and Practice. World Scientific, New Jersey.

Edelman, T., 1968. Dune erosion during storm conditions. In: Proceedings of the 11th International Conference on Coastal Engineering. ASCE, New York,

pp. 719–722.

Edelman, T., 1972. Dune erosion during storm conditions. In: Proceedings of the 13th International Conference on Coastal Engineering. ASCE, New York, pp. 1305–1312.

Edge, B.L., Ewing, L., Erickson, K.M., Magoon, O.T., 2003. Application of Coastal Engineering in Coastal Zone Management. In: Advances in Coastal Structures Design. ASCE, pp. 200–215.

El Mrini, A., Anthony, E.J., Maanan, M., Taaouati, M., Nachite, D., 2012. Beach-dune degradation in a Mediterranean context of strong development pressures, and the missing integrated management perspective. Ocean Coast. Manag. 69, 299–306.

Erikson, L.H., Larson, M., Hanson, H., 2007. Laboratory investigation of beach scarp and dune recession due to notching and subsequent failure. Marine Geology 245, 1–19.

Feagin, R.A., Williams, A.M., Popescu, S., Stukey, J., Washington-Allen, R.A., 2014. The use of terrestrial laser scanning (TLS) in dune ecosystems: the lessons learned. J. Coast. Res. 30 (1), 111–119.

Fewtrell, T.J., Duncan, A., Sampson, C.C., Neal, J.C., Bates, P.D., 2011. Benchmarking urban flood models of varying complexity and scale using high resolution terrestrial LiDAR data. Phys. Chem. Earth 36 (7–8), 281–291.

Figlus, J., Kobayashi, N., Gralher, C., Iranzo, V., 2011. Wave overtopping and overwash of dunes. J. Waterw. Port, Coast. Ocean Eng. 137 (1), 26–33.

Fisher, J.S., Overton, M.F., 1985. Numerical model for dune erosion due to wave uprush. In: Proceedings of the 19th International Conference on Coastal Engineering. ASCE, New York, pp. 1107–1115.

Flick, R.E., 1993. The myth and reality of southern California beaches. Shore Beach 61 (3), 3–13.

Flick, R.E., 1998. Comparison of California tides, storm Surges and mean sea level during the En niño winters of 1982–83 and 1997–98. Shore Beach 66 (3), 7–11.

Froede, C.R., 2010. Constructed sand dunes on the developed barrier-spit portion of Dauphin Island, Alabama. J. Coast. Res. 26 (4), 699–703.

Gallien, T.W., Schubert, J.E., Sanders, B.F., 2011. Predicting tidal flooding of urbanized embayments: a modeling framework and data requirements. Coast. Eng. 58 (6), 567–577.

Gallien, T.W., Sanders, B.F., Flick, R.E., 2014. Urban coastal flood prediction: integrating wave overtopping, flood defenses and drainage. Coast. Eng. 91, 18–28.

Gares, Paul A., Wang, Yong, White, Stephen A., 2006. Using LIDAR to monitor a beach nourishment project at Wrightsville Beach, North Carolina, USA. J. Coast. Res. 1206–1219.

Guza, R.T., Feddersen, F., 2012. Effect of wave frequency and directional spread on shoreline runup. Geophys. Res. Lett. 39, L11607.

Hanley, M.E., Hoggart, S.P.G., Simmonds, D.J., Bichot, A., Colangelo, M.A., Bozzeda, F., Heurtefeux, H., Ondiviela, B., Ostrowski, R., Recio, M., Trude, R., Zawadzka-Kahlau, E., Thompson, R.C., 2014. Shifting sands? Coastal protection by sand banks, beaches and dunes. Coast. Eng. 87, 136–143.

Hanson, H., Brampton, A., Capobianco, M., Dette, H.H., Hamm, L., Laustrup, C., et al., 2002. Beach nourishment projects, practices, and objectives a European overview. Coast. Eng. 47, 81–111.

Hanson, S., Nicholls, R., Ranger, N., Hallegatte, S., Corfee-Morlot, J., Herweijer, C., Chateau, J., 2011. A global ranking of port cities with high exposure to climate extremes. Clim. Change 104, 89–111.

Hapke, C.J., Reid, D., Richmond, B., 2009. Rates and trends of coastal change and regional behavior of the beach and cliff system. J. Coast. Res. 25 (3), 603–615.

Harley, M.D., Ciavola, P., 2013. Managing local coastal inundation risk using real-time forecasts and artificial dune placements. Coast. Eng. 77, 77–90.

Judge, E.K., Overton, M.F., Fisher, J.S., 2003. Vulnerability indicators for coastal dunes. J. Waterw. Port Coast. Ocean Eng. 129 (6), 270–278.

Kana, T.W., Svetlichny, M., 1982. Artificial manipulation of beach profiles. In: Proceedings of the 18th Coastal Engineering Conference, pp. 903–922.

Kobayashi, N., 1987. Analytical solution for dune erosion by storms. J. Waterw. Port. Coast. Ocean Eng. 113 (4), 401–418.

Kratzmann, M.G., Hapke, C.J., 2012. Quantifying anthropogenically driven morphologic changes on a barrier island: fire island national Seashore, New York. J. Coast. Res. 28 (1), 76–88.

Kriebel, D.L., 1991. Advances in numerical modeling of dune erosion. In: Proceedings of the 22nd International Conference on Coastal Engineering. ASCE, New York, pp. 2305–2317.

Kriebel, D.L., Dean, R.G., 1985. Numerical simulation of time dependent beach and dune erosion. Coast. Eng. 9, 221–245.

Larson, M.L., Kraus, N.C., 1989. SBEACH: Numerical Model for Simulating Storm-induced Beach Change, Report 1. Empirical Formulation and Model Development. US Army Corps of Engineering, Vicksburg, MS.

Larson, M., Erikson, L., Hanson, H., 2004. An analytical model to predict dune erosion due to wave impact. Coast. Eng. 54, 675–696.

Laudier, N.A., Thorntorn, E.B., MacMahan, J., 2011. Measured and modeled wave overtopping on a natural beach. Coast. Eng. 58, 815–825.

Linham, M.M., Nicholls, R.J., 2012. Adaptation technologies for coastal erosion and flooding: a review. Marit. Eng. 165 (MA3), 95–111.

Magliocca, N.R., McNamara, D.E., Murray, A.B., 2011. Long-term large-scale morphodynamic effects of artificial dune construction along a barrier island Coastline. J. Coast. Res. 27 (5), 918–930.

Malibu Times, June 15, 2005. Broad Beach Sand Battle Results in Denials, Outrage. Available at: http://www.malibutimes.com/news/article_4ab144cf-75b3-5144-84b0-f41a6f33901d.html.

Martin, D., Bertasi, F., Colangelo, M.A., de Vries, M., Frost, M., Hawkins, S.J., Macpherson, E., Moschella, P.S., Satta, M.P., Thompson, R.C., Ceccherelli, V.U., 2005. Ecological impact of coastal defence structures on sediment and mobile fauna: evaluating and forecasting consequences of unavoidable modifications of native habitats. Coast. Eng. 52, 1027–1051.

Matias, A., Ferreira, O., Mendes, I., Dias, J.A., Villa-Concejo, A., 2005. Artificial construction of dunes in the south of Portugal. J. Coast. Res. 21 (3), 472–481.

McMahon, T., 2009. Nourishment in Seal Beach 2009-Efficiencies in Addressing Sediment Loss, Presented Headwaters to Oceans (H_2O). Available at: http://www.coastalconference.org/h20_2009/pdf/2009presentations/2009-10-27-Tuesday/Session.

McNinch, J.E., Wells, J.T., 1992. Effectiveness of Beach scraping as a method of erosion control. Shore Beach 60 (1), 13–20.

Moreno, R., February 21, 2013. SANDAG Discourages Lawsuits in Update on City Sand Project Ponding. Imperial Beach Patch. Available at: http://imperialbeach.patch.com/groups/politics-and-elections/p/seacoast-residents-pound-sandag-on-sand-project-ponding.

National Oceanic and Atmospheric Administration (NOAA). NOAA Tides and Currents (accessed 06.03.13.), Available at: http://tidesandcurrents.noaa.gov/.

National Research Council, 2012. Sea-level Rise of the Coasts of California, Oregon and Washington: Past, Present, and Future. National Academies Press, Washington DC.

National Research Council, Marine Board, 1995. Beach Nourishment and Protection. National Academies Press, Washington, DC.

Nicholls, R.J., 2011. Planning for the impacts of sea level rise. Oceanography 24 (2), 144–157.

O'Reilly, W.C., Guza, R.T., 1991. Comparison of spectral refraction and refraction-diffraction wave models. J. Waterw. Port. Coast. Ocean. Eng 117 (3), 199–215.

O'Reilly, W.C., Guza, R.T., 1993. A comparison of two spectral wave models in the southern California Bight. Coast. Eng. 19, 263–282.

O'Reilly, W.C., Guza, R.T., 1998. Assimilating coastal wave observations in regional swell predictions. Part I: Inverse methods. J. Phys. Oceanogr. 28 (4), 679–691.

Overton, M.F., Fisher, J.S., Hwang, K., 1994. Development of a dune erosion model using SUPERTANK data. In: Proceedings of the 24th International Conference on Coastal Engineering. ASCE, pp. 2488–2502.

Pendleton, L., Mohn, C., Vaughn, R.K., King, P., Zoulas, J.G., 2012. Size matters: the economic value of beach erosion and nourishment in southern California. Contemp. Econ. Policy 30 (2), 223–237.

Pietro, L.S., O'Neal, M.A., Puleo, J.A., 2008. Developing terrestrial-lidar based digital elevation models for monitoring beach nourishment performance. J. Coast. Res. 24 (6), 1555–1564.

Roelvink, D., Reniers, A., van Dongeren, A., de Vries, J.V.T., McCall, R., Lescinski, J., 2009. Modelling storm impacts on beaches, dunes and barrier islands. Coast. Eng. 56 (11–12), 1133–1152.

Rogers, J., Hamer, B., Brampton, A., Challinor, S., Glennerster, M., Brenton, P., Bradbury, A., 2010. Beach management Manual, second ed. CIRIA, London, UK.

Sallenger, A.H., 2000. Storm impact scale for barrier islands. J. Coast. Res. 16 (3), 890–895.

Sallenger Jr., A.H., Krabill, W.B., Swift, R.N., Brock, J., List, J., Hansen, M., Holman, R.A., Manizade, S., Sontag, J., Meredith, A., Morgan, K., Yunkel, J.K., Frederick, E.B., Stockdon, H., 2003. Evaluation of airborne topographic lidar for quantifying beach changes. J. Coast. Res. 19 (1), 125–133.

Sanders, B.F., 2007. Evaluation of on-line DEMs for flood inundation modeling. Adv. Water Resour. 30, 1831–1843.

Schubert, J.E., Gallien, T.W., Shakeri Majd, M., Sanders, B.F., (in press). Terrestrial laser scanning of anthropogenic beach berm erosion and overtopping. J. Coast. Res.. DOI: 10.2112/JCOASTRES-D-14-00037.1.

Stockdon, H.F., Doran, K.S., Sallenger, A.H., 2002. Extraction of lidar-based dune-crest elevations for use in examining the vulnerability of beaches to inundation during Hurricanes. J. or Coast. Res. SI53, 59–65.

Stockdon, H.F., Holman, R.A., Howd, P.A., Sallenger, A.H., 2006. Empirical parameterization of setup, swash and runup. Coast. Eng. 53, 573–588.

Surfside Colony, 2012. Welcome Surfside Colony Residents!. Available at: http://www.surfsidecolony.org/.

Tye, R.S., 1983. Impact of Hurricane David and mechanical dune restoration on Folly Beach, South Carolina. Shore Beach 51 (2), 3–9.

United States Army Corps of Engineers (USACE), 2002. Coast of California Storm and Tidal Waves Study, South Coast Region, Orange County: Final Report.

van de Graff, J., 1977. Dune erosion during a storm surge. Coast. Eng. 1, 99–134.

van Rijn, L., 2009. Prediction of dune erosion due to storms. Coast. Eng. 56 (4), 441–457.

van Rijn, L., 2011. Coastal erosion and control. Ocean Coast. Manag. 54, 867–887.

Vellinga, P., 1982. Beach and dune erosion during storms. Coast. Eng. 3, 361–387.

Wells, J.T., McNinch, J., 1991. Beach scraping in North Carolina with special reference to its effectiveness during Hurricane Hugo. J. Coast. Res. 8, 249–261.

Yates, M.K., Guza, R.T., O'Reilly, W.C., Seymour, R.J., 2009. Overview of seasonal sand level changes on southern California beaches. Shore Beach 77 (1), 39–46.

Young, A.P., Ashford, S.A., 2006. Application of airborne LiDAR for Seacliff Volumetric change and Beach-Sediment Budget contributions. J. Coast. Res. 22, 307–318.

Young, A.P., Guza, R.T., O'Reilly, W.C., Flick, R.E., Gutierrez, R., 2011. Short-term retreat statistics of a slowly eroding coastal cliff. Nat. Hazards Earth Syst. Sci. 11, 205–217.